

Acquisition-Weighted Stack of Spirals for High-Resolution Sodium MRI

Y. Qian¹, F. Boada¹

¹Radiology, University of Pittsburgh, Pittsburgh, PA, United States

INTRODUCTION

One common limitation for efficient sodium MRI in human is the high slew rate required for efficient trajectory designs such as twisted projection imaging (TPI) (1). The slew rate constraint often leads to lower resolution images than what could be achieved given the available signal-to-noise ratio (SNR). In this work, we demonstrate a new strategy for sodium MRI data acquisition, acquisition-weighted stack of spirals (AWSOS), which exploits fast evolving spiral trajectories (2) and variable acquisition delay (3) to address the constraints imposed by sodium's fast T_2 decay. The AWSOS is capable of achieving high in-plane resolution (up to 1mm) while keeping the data acquisition time relatively short. Numerical models and phantoms will be used to illustrate the feasibility of the AWSOS method.

METHODS AND MATERIALS

Three main features are used to establish the AWSOS method (Fig. 1). First, a soft rf pulse associated with a slab select gradient was used to replace the non-selective hard rf pulse used in current TPI sequences. Second, the duration of the slice encoding gradient is allowed to vary flexibly, leading to a variable acquisition delay. Short durations are assigned to low phase values while long durations are for high phase values (3). Third, interleaved spirals are used to speed up readout and to reduce the number of in-plane encodings.

The optimal length of single spiral leaf was investigated on a numerical model (a cylinder with varying diameter rods, $T_2=3\text{ms}$). The number of interleaves was evaluated for matrix sizes, $64 \times 64 \times 30$ and $128 \times 128 \times 30$, at $\text{FOV}=22 \times 22 \times 15\text{cm}^3$. The k-space data including the T_2 decay during the slice encoding and spiral evolution were analytically calculated along the spirals with $4\mu\text{s}$ sampling interval. Images were reconstructed using the gridding algorithm. Phantom studies were performed on proton phantoms on a 3T scanner (GE Signa CV/i, Milwaukee, WI, $G_{\text{max}}=40\text{mT/cm}$ & $S_{\text{max}}=150\text{T/m/s}$) using a GE standard head coil. A sinc pulse of 0.4ms duration was used to excite a 15cm-thick slab with $\text{TE/TR} = 0.408/100\text{ms}$. There were 30 slice encodings (i.e. 5mm slice thickness). An in-plane FOV of $14 \times 14\text{cm}^2$ was used to evaluate the performance of the approach at higher resolutions.

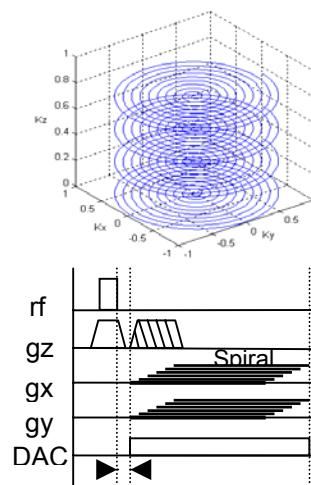


Fig.1. Stack of spirals (top) and AWSOS sequence diagram (bottom).

RESULTS AND DISCUSSIONS

The optimal short readouts for the shortest total acquisition time are summarized in Tab.1 (in boldface). For a resolution of 2.2mm (64×64 matrix), for instance, we used 8 spirals with 7.344ms readout. Simulated high-resolution images are shown in Fig.2.

The short T_2 decay had a smaller effect on the spatial resolution when short spirals were used (rightmost column, Fig. 2). It was also found that there was not much difference (18%) in intensity between 8 and 16 leaves for a 64×64 matrix and (3%) between 12 and 24 leaves for a 128×128 matrix. Consequently, the optimal choice for $\text{FOV}=22\text{cm}$ was 8 leaves (5.248ms readout) for 3.4mm resolution or 12 leaves (11.800ms) for 1.7mm resolution. Phantom images are shown in Fig. 3. Three in-plane resolutions (2.2, 1.1, and 0.55mm) were achieved with readout times of 7.344ms (64×64), 13.612ms (128×128), and 34.860ms (256×256), respectively. The total number of excitations (without averaging) was 240, 480, and 720, respectively, which was substantially smaller than those required for 3D radial projections or even in the TPI sampling scheme for the same spatial resolution. Overall, our results indicate that the AWSOS is capable of high spatial resolution in shorter imaging times than some of the previously described techniques without a significant degradation in image quality.

Tab.1. Spiral parameters at $\text{FOV}=22\text{cm}/14\text{cm}$

Matrix size	In-plane resolution (mm)	Spiral leaf	Readout (ms)
64×64	3.4/2.2	4	10.100/14.136
		8	5.248/7.344
		16	2.940/4.056
128×128	1.7/1.1	6	23.068/35.076
		12	11.800/17.880
		16	9.024/13.612
		24	6.276/9.372
256×256	0.9/0.55	24	22.496/34.860

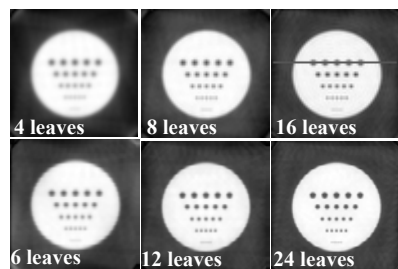


Fig.2. Simulation images for matrix size 64×64 (top) and 128×128 (bottom). $T_2=3\text{ms}$ and $\text{FOV}=22\text{cm}$.

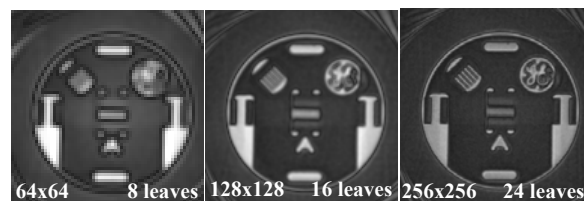


Fig.3. Phantom images for matrix size 64×64 , 128×128 , and 256×256 at $\text{FOV}=14\text{cm}$.

REFERENCES

- Boada FE, et al. Magn Reson Med 1997; 37:706-715.
- Glover GH. Magn Reson Med 1999; 42:412-415.
- Robson MD, et al. Magn Reson Med 2005; 53:267-274.